Flow structure over rolling-grain ripples – laboratory experiments and theoretical study

H.N. Yoshikawa(1), G. Rousseaux(2), J. Kruithof(1), A. Stegner(3), & J.E. Wesfreid(1)

(1) Physique et Mécanique des Milieux Hétérogènes, UMR7636 CNRS-ESPCI, 10, rue Vauquelin 75231 Paris Cedex 05 France, e-mail: harunori@pmmh.espci.fr
(2) Institut Non-Linéaire de Nice, UMR 6618 CNRS, e-mail: Germain.Rousseaux@inln.cnrs.fr
(3) Laboratoire de Météorologie Dynamique, ENS-Paris

Abstract

Oscillatory shear at a flat sand-water interface can make the interface be instable and lead to wavy patterns as we see in shallow coastal regions. At the first stage of this instability appear gentle small ripples accompanied by grains rolling along the interface, *rolling-grain ripples*, which always evolve to higher sharp ripples (*vortex ripples*). We determine fluid-flow structure above rolling-grain ripples by PIV (Particle Image Velocimetry) measurements and find transient eddies on ripple troughs. Perturbative calculation method for the flow over rigid wavy wall predicts the similar structure and application of that method to Stokes equation concludes that observed eddies are created by viscous effect.

1. Introduction

1.1 Introduction

On seabed in shallow coastal regions, there are often regular ripple patterns, which are considered as created by back and forth motion of water near the bed. Since the seminal work of Bagnold (1946), two types of ripples have been distinguished: *rolling-grain ripples* and *vortex ripples*. The rolling-grain ripples are gentle small ripples on which sand grains roll back and forth along the sand-water interface in the same direction as the water oscillatory motion near the bed. This type of ripples was recently shown to always evolve and, after a transition, switch to the vortex ripples (Stegner (1999)). The vortex ripples are larger sharp structure accompanied by vortices which detach from the crests to take and put grains from the crests to the neighboring structure.

About the flow over rolling-grain ripples, there are some works trying to predict the flow by means of the perturbative method. Within short or long wave limit, Lyne (1971) predicted that waviness of a small rigid wavy bottom modifies a simple oscillatory Stokes flow above a flat bottom and creates the flow component independent of time, *steady streaming*. He found that the steady streaming has a structure consisting of even number cells with closed streamlines which have the direction from the trough to the crest at the bottom. Other researchers arrived at the similar results for different parameter regime or with higher accuracy (Sleath (1976), Kaneko and Honji (1979), Matsunaga et al. (1981), Vittori (1989), Blondeaux (1990), Hara and Mei (1990), Hara et al. (1992)). It is considered that averaged shear of the steady streaming would be the origin of the rolling-grain ripple formation. Kaneko & Honji (1979) performed experiments using glycerin-water solution and shadowgraph techniques to found cellular patterns resembling the steady streaming. Among the above theoretical works, those of Vittori (1989), Blondeaux (1990) and Hara et al. (1992) are applicable to real rolling-grain ripple case, for which the wavelength l is of the same order as the amplitude A of water oscillation. Blondeaux (1990) and Vittori & Blondeaux (1990) combined perturbatively determined steady streamings and empirical law of sand transport to model the generation and evolution of rolling-grain ripples, respectively.

In the present study, we visualize instantaneous flow structure above real rolling-grain ripples making of use the PIV technic (section 2), which has never been performed to our knowledge. To compare the obtained results with theoretical prediction of an existing theory, transient structure is calculated (section

3). In the section 4, very good agreements between experiments and theory are described and another theoretical calculation is performed to examine the origin of observed flow structure.

2. Experiments

2.1 Set-up and technics

Sand (monodisperse spherical glass beads, diameter $110\mu m$) and water are contained between two concentric Plexiglas cylinders (mean radius $13.6cm$, gap size $2.5cm$, see (Fig. 1)) and this container is oscillated at specified amplitude and frequency by a brushless motor around the axis azimuthally. A laser diode ($685nm$, $50mW$) is fixed above the container and lights up the sand-water interface. Plastic powder (ORGASOL, diameter $60\mu m$, density $1.03 g/cm^3$) is seeded in water and the light scattered by the powder particles is captured by a CCD camera (250 images per second). The laser diode and the CCD camera oscillate azimuthally together with the container. Images taken by the camera are stored in a personal computer and velocity field of fluid is determined from these stored data. From the determined velocity field, the field of stream function, vorticity, etc. can be calculated.

Each run of experiments is started from a flat weakly-compacted sand-water interface which is prepared by the preliminary steps such that: strong oscillations of the container to fluidize sand bed, and rapid diminution and stop of the oscillation to settle down suspended sand-grains. These steps enable to obtain a uniform initial condition and bring about reproducibility to experiments.

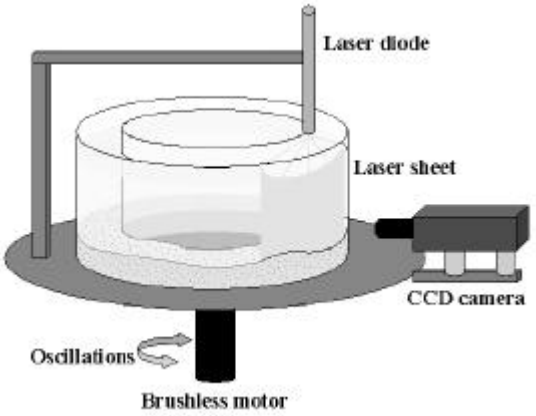

Fig. 1 – Experimental set-up (schematic diagram)

2.2 Results

An example of determined flow above rolling-grain ripples is shown in the left column of Fig. 2, a series of flow streamline images, where the interval between images is $0.008 s$ and the ambient flow goes from the left to the right except in the last image (ambient flow stops). Experimental parameters are: water oscillation amplitude A=1.5 cm, frequency $f=1 s^{-1}$, the number of oscillation N_{osci}=1620 which is counted from the beginning of the run. As seen in the figure, cellular structure is observed, which only exists during each flow reversal and, for the other moments, only simple shear flow is seen. It is seen that, before the ambient flow stops, closed structure occupying whole a ripple trough enlarges vertically and then shrinks rapidly during the interval between the second and third images.

3. Numerical resolution

3.1 Summary of stream function determination

According to Vittori (1989), the flow oscillating along the wave vector of a bottom wavy pattern is given by the following streamfunction within the first order approximation with respect to the ripple height :

$$y = y\cos(t) + \frac{1}{\sqrt{2}} e^{-y} \cos(t - y - p/4) + \frac{e}{2}\left[\sum_{m=-\infty}^{\infty} G_m(y) e^{imt} e^{i(ax - pr\sin t)} + c.c. \right], \quad (1)$$

where x and y are horizontal and vertical coordinates, respectively. y axis is taken upper wards and, in this coordinate system, the bottom surface has an expression of $y = e\cos(ax)$. Both x and y are

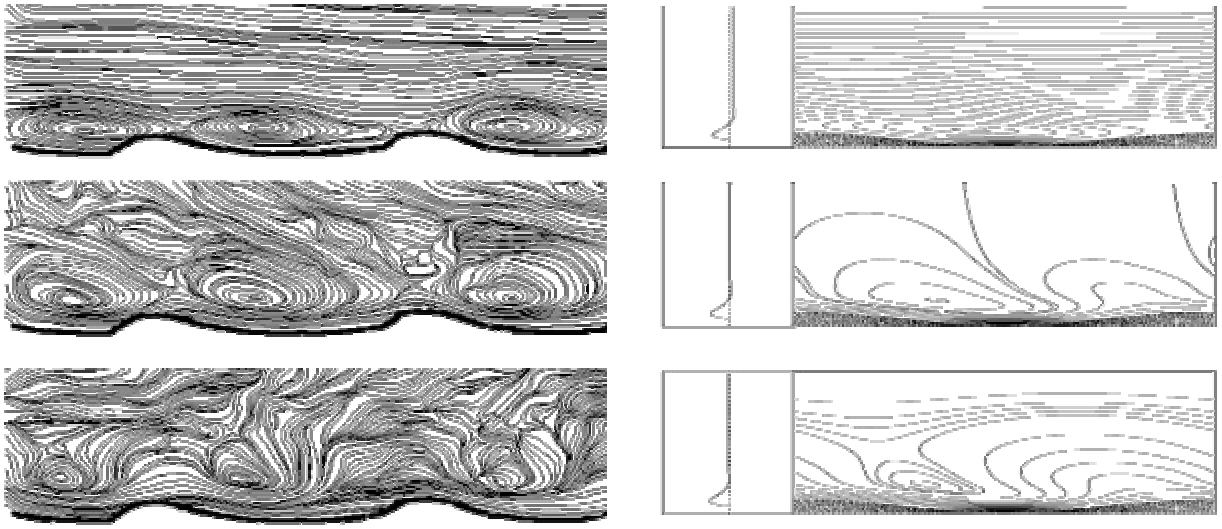

Fig. 2 – Comparison of the experimentally observed and theoretically predicted flow structures: streamlines captured by PIV measurement (left column) and calculated by perturbative method (right column). The interval between rows is 0.008 s. The middle row corresponds to the flow reversal moment from the right to the left.

measured in d (Stokes boundary layer thickness defined as $d = \sqrt{n/p\mathrm{f}}$). The time t is measured in $T/2p$ and the streamfunction y in $2p\mathrm{f}Ad$. Unknown functions $G_m(y)$ should be determined by the following ordinary differential equation set:

$$(D^2 - a^2)(D^2 - a^2 - i2m)G_m = ipr\left[e^{-(1+i)y}(D^2 - a^2 - i2)G_{m-1} + e^{-(1-i)y}(D^2 - a^2 + i2)G_{m+1}\right], \quad (2)$$

under the boundary conditions:

$$(DG_m)_{y=0} = -\frac{1+i}{2} J_{m-1}(pr) - \frac{1-i}{2} J_{m+1}(pr), \quad (G_m)_{y=0} = 0, \quad (DG_m)_{y\to\infty} = 0, \quad (G_m)_{y\to\infty} = 0, \quad (3)$$

where r is the Keulegan-Carpenter number defined by $r = 2A/l$ and $J_m(x)$ is the first kind Bessel function of order m.

After the truncation of the infinite series on the left hand side of (1), the finite equation set reduced from Eq. (2) can be integrated from a sufficiently high position with unknown constants, which are determined by the boundary condition at $y = 0$.

3.2 Results

Calculated flow also has transient structure that only appears during flow reversal. For the parameter regime within which we generated natural ripples in laboratory experiments and observed upper flow structure, the calculation predicts the appearance of a transient eddy over each ripple trough during each flow reversal. Around $1/8$ period before the flow reversal moment, these eddies are generated at the lee side of the ripples and ejected from the troughs, growing rapidly in their vertical size. After the reversal moment, the eddies shrink quickly and disappear within a very short time, and then only simple shear flow

structure along the wavy bottom is observed until the next flow reversal. An example of predicted flow evolution during the flow reversal is presented in the right column of Fig. 2. Parameters are matched to those for the experiment shown in the left column. Any neighbors in the figure correspond to the same moment. On the left of each predicted flow image, the profile of unperturbed Stokes flow at the same time is also plotted.

4. Discussion

As seen in Fig. 2, the perturbative calculation can predict very well the flow structure above rolling-grain ripples. About the form of the eddies and its evolution, a very good agreement is seen between the left and right columns in the figure. For more quantitative comparison, the displacement of the eddy's center is plotted in Fig. 3. Time origin is taken at the flow reversal moment from the right to the left. Parameter values are the same as Fig. 2 except for the dotted lines, which corresponds to smaller ripple case (e=0.1). In the figure, null velocity position of the Stokes flow is also plotted by a dashed line.

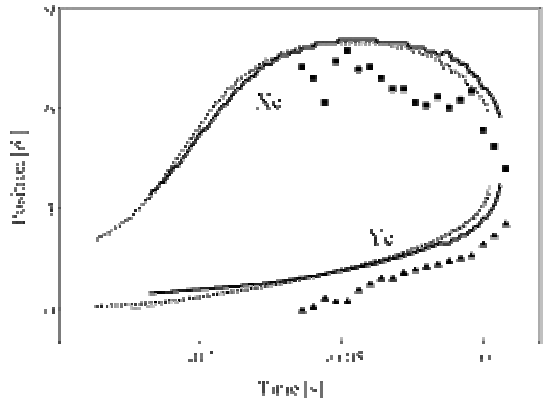

Fig. 3 – Displacement of eddy's center : A=1.5 cm, f =1 Hz, l =1.2 cm, and h=1.1 mm (for solid lines and experimental datum) or h=0.11 mm (for dotted lines). Other parameters for experiments : d=110 μm and N_{osci}=1620 . Time origin is taken at the flow reversal moment.

A very good agreement is also observed in this figure. Main tendencies are the same in the experimental data and in the theoretical prediction. From theoretical curves, it is easily seen that the eddy's center motion depends little on the ripple height. Furthermore, Y_C evolution goes almost along the null velocity position of the unperturbed Stokes flow. It could imply that the perturbative term of Eq.(1) is small even if the ripple height is not small compared with Stokes layer thickness, at least above the y=0 plane. This implication squares with the good agreement seen in Fig. 2.

To identify the origin of the observed eddies, we perform another theoretical approach, neglecting non-linear term in Navier-Stokes equation. In this case, there are non interaction between different modes G_m because the non-linear term corresponds to the right hand side of Eq.(2) which represents the interactions. The solution $G_m'(y)$ for this case is easily written analytical form :

$$G_m'(y)=\frac{e^{ip/4}J_{m-1}(pr)+e^{-ip/4}J_{m+1}(pr)}{\sqrt{2}\left[(1-d_m)(a_m-a)-d_m\right]}\cdot\left[(1-d_m)\left(e^{-a_m y}-e^{-ay}\right)+yd_m e^{-a_m y}\right], \qquad (4)$$

where $a_m=\sqrt{a^2+i2m}$ and d_m=1 (m=0) or 0 ($m\neq0$).

As shown in the Fig. 4, flow structure predicted by this solution resembles much to the eddy discussed above, although the center of the structure is shifted downstream a little. This could bring us an assertion that experimentally observed eddies above rolling-grain ripples come mainly from viscous effect and

inertial effect represented by the non-linear term of Navier-Stokes equation does not play important role for such structure. The transition of flow structure from viscous eddies above rolling-grain ripples to vortices above vortex ripples reminds us the transition of flow behind a backward-facing step, in which a purely viscous structure at low Reynolds number (Moffatt (1964)) is displaced by a vortex accompanied by a boundary layer separation for higher Reynolds number (Alleborn (1997)).

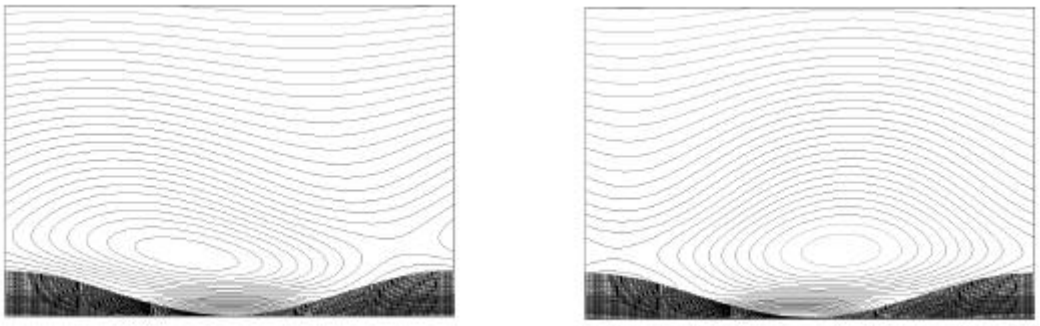

Fig. 4 – Flow patterns with (left) or without (right) the non-linear term : 20 ms before the flow reversal (from the right to the left), $\Delta y = 0.06$. Other parameters are the same as Fig. 2.

5. Conclusion

We were able to see for the first time the flow pattern, especially transient eddies, above naturally generated rolling-grain ripples. The morphological evolution of the flow structure is well predicted by the theory on the flow above a rigid sinusoidal wavy wall, which only takes into account the first order correction proportional with respect to the ripple height. To examine the solutions of Stokes equation revealed that these eddies are created by viscous effect and imply an analogy between the transitions of flow structure over sand ripples and behind a backward-facing step.

References

Alleborn, N., Nandakumar, K., Raszillier, H. and Durst, F., Further contributions on the two-dimensional flow in a sudden expansion, *J. Fluid. Mech.*, Vol. 330, pp. 169-188, 1997.

Bagnold, R.A., Motion of waves in shallow water Interaction between waves and sand bottoms. With an additional note by Sir G.I. Taylor, Proc. R. Soc. London, Ser. A, Vol. 187, pp. 1-15, 1946.

Blondeaux, P., Sand ripples under sea-waves. Part 1. Ripple formation., *J. Fluid. Mech.*, Vol. 218, pp. 1-17, 1990.

Faraci, C. and Foti, E., Evolution of small scale regular patterns generated by waves propagating over a sandy bottom, *Phys. Fluids*, Vol. 13(6), pp. 1624-1634, 2001.

Kaneko, A. and Honji, H., Double structures of steady streaming in the oscillatory viscous flow over a wavy wall, *J. Fluid. Mech.*, Vol. 93, pp. 727-736, 1979.

Hara, T. and Mei, C.C., Oscillating flow over periodic ripples, *J. Fluid. Mech.*, Vol. 211, pp. 183-209, 1990.

Hara, T., Mei, C.C. and Shum, K.T., Oscillatory flow over periodic ripples of finite slope, *Phys. Fluids A*, Vol. 4(7), pp. 1-12, 1992.

Honji, H., Kaneko, A. and Matsunaga, N., Flow above oscillatory ripples, *Sedimentology*, Vol. 27, pp. 225-229, 1980.

Lyne, W.H., Unsteady viscous flow over a wavy wall, *J. Fluid. Mech.*, Vol. 50, pp. 33-48, 1971.

Matsunaga, N., Kaneko, A. and Honji, H., A numerical study of steady streamings in the oscillatory flow over a wavy wall, *J. Hydraul. Res.*, Vol. 19(1), pp. 29-42, 1981.

Moffatt, H.K., Viscous and resistive eddies near a sharp corner, *J. Fluid. Mech.*, Vol. 18, pp. 1-18, 1964

Scherer, M.A., Melo, F. and Marder, M., Sand ripples in an oscillating sand-water cell, *Phys. Fluids*, Vol. 11(1), pp. 58-67, 1999.
Sleath, J.F.A., On rolling-grain ripples, *J. Hydraul. Res.*, Vol. 14(1), pp. 69-81, 1976.
Sleath, J.F.A., *Sea bed mechanics*, Wiley, 1984.
Stegner, A. and Wesfreid, J.E., Dynamical evolution of sand ripples under water, *Phys. Rev. E,* Vol. 60(4), pp. 3487-3490, 1999.
Vittori, G., Non-linear viscous oscillatory flow over a small amplitude wavy wall, *J. Hydraul. Res.*, Vol. 27(2), pp. 267-280, 1989.
Vittori, G. and Blondeaux, P., Sand ripples under sea-waves. Part 2. Finite-amplitude development., *J. Fluid. Mech.*, Vol. 218, pp. 19-39, 1990.